



## Supporting Information

for *Small*, DOI: 10.1002/smll.201900046

Adhesive Hemostatic Conducting Injectable Composite  
Hydrogels with Sustained Drug Release and Photothermal  
Antibacterial Activity to Promote Full-Thickness Skin  
Regeneration During Wound Healing

*Yongping Liang, Xin Zhao, Tianli Hu, Baojun Chen, Zhanhai  
Yin, Peter X. Ma, and Baolin Guo\**

## Supporting Information

### **Adhesive hemostatic conducting injectable composite hydrogels with sustained drug release and photo-thermal antibacterial activity to promote full-thickness skin regeneration during wound healing**

Yongping Liang, Xin Zhao, Tianli Hu, Baojun Chen, Zhanhai Yin, Peter X. Ma, and Baolin Guo\*

#### **Materials and methods**

##### **Synthesis of hyaluronic acid–dopamine (HA-DA)**

To prepare the hyaluronic acid–dopamine conjugate, HA (1 g, 2.5 mmol) was dissolved in 100 mL of degassed deionized water, and the solution was kept under nitrogen. EDC (575 mg, 3 mmol) and NHS (345 mg, 3 mmol) were slowly added to the solution. After 20 min stirring, dopamine hydrochloride (569 mg, 3 mmol) was added to the mixture. The pH value of the solution was monitored and adjusted to keep the value between 5 and 6 for 3 h by adding 0.1 N hydrochloric acid and NaOH. Subsequently, the solution was allowed to react overnight at room temperature. And after the reaction, the solution was purified by dialysis (MWCO = 10,000 Da) for 3 days under acidic conditions and lyophilized. The resulting white foam was stored at  $-20\text{ }^{\circ}\text{C}$  before use. The catechol content was confirmed by UV–vis spectrometer (PerkinElmer Lambda 35), measuring absorbance at 280 nm, and quantitative measurement was performed with a dopamine standard. The degree of dopamine substitution for HA-DA was 12 %. In addition, nuclear magnetic resonance (NMR) analysis was performed (Bruker 400 MHz, Bruker, Billerica, MA) with the  $^1\text{H}$  NMR spectrum of  $\text{D}_2\text{O}$  at 4.74 ppm as reference.

##### **Synthesis of polydopamine coated GO (rGO@PDA)**

GO (20 mg) and dopamine hydrochloride (20 mg) were dissolved in 40 mL Tris–HCl buffer

(pH = 8.5) and sonicated for 30 min. The mixture was stirred vigorously for 24 h at room temperature. The resulting mixture was purified and separated by filtration and further washed with water and ethanol several times to obtain the rGO@PDA composite. Finally, the rGO@PDA was dried in a vacuum oven at 60 °C for 48 h.<sup>[1, 2]</sup>

### **Scanning electron microscope (SEM)**

After all the hydrogel samples were sprayed with a thin gold layer, the morphologies of freeze-dried hydrogels were examined by a field emission scanning electron microscope (FE-SEM; QUTAN FEG 250, FEI). NIH Image J software was employed to measure the pore diameters of hydrogel samples. For each hydrogel sample (at least 3 samples), every hydrogel had four pictures taken from various regions of the hydrogel. Every picture was measured by more than five pores. We then processed the above data using one-way ANOVA followed by Bonferroni post hoc test to determine the statistical differences (\*p < 0.05).

### **Thermal stability of GO and rGO@PDA**

The thermal stability of GO and rGO@PDA were tested by thermogravimetric analysis (TGA) using a Mettler-toledo TGA thermogravimetric analyzer under a nitrogen atmosphere (nitrogen flow rate 50 mL min<sup>-1</sup>) and a heating rate of 10 °C min<sup>-1</sup>. The scan range was between 30 and 700 °C.<sup>[3]</sup>

### **Swelling test**

Swelling test was used to determine the swelling ratio (SR) and stability of the hydrogels. The completely gelled wet hydrogels were put into 20 mL PBS (0.01 M pH 7.4) in sealed vials at 37 °C. When reaching the pre-set time interval, the hydrogels were taken out from the solution and the superficial water was removed using a filter paper. Following that, the hydrogels were weighed. The test was not finished until the weight of all hydrogel kept constant. SR was calculated using the following equation:  $SR = (W_t - W_0) / W_0 \times 100\%$ , where  $W_0$  and  $W_t$  represented the initial weight of the wet hydrogels and the weight after swelling pre-set time, respectively. The test was repeated three times.<sup>[4]</sup>

### **In vitro degradation test**

For the in vitro degradation test, hydrogel bulks, with the same volume, were immersed in 30 mL PBS (pH =7.4) at constant temperature (37 °C) with shaking at 100 rpm, respectively. At the predetermined time point, hydrogel samples were taken out and rinsed with DI water to remove excess salinity, they were then dried in an oven at 60 °C for 48 h and weighed. The weight remaining ratio % of hydrogels was then defined by the following equation:

Weight remaining ratio of hydrogel (%) =  $(W_t - W_0) / W_0 \times 100\%$ , where  $W_t$  and  $W_0$  are the dry weight of the remaining hydrogels after degradation at different time points and the dry weight of the initial hydrogels, respectively.<sup>[5]</sup>

### **Self-healing performance of hydrogels**

The hydrogel disks were prepared with a 20 mm diameter and 1 mm height. Using the strain amplitude sweep method ( $\gamma$  from 1% to 2000%), the value of the critical strain region was recorded. Then the other hydrogel disks were employed to test the self-healing behaviors by alternate strain sweep test at a fixed angular frequency ( $1 \text{ rad}\cdot\text{s}^{-1}$ ). Amplitude oscillatory strains were switched from small strain ( $\gamma = 1.0\%$ , 60 s for each interval) to large strain ( $\gamma = 2000\%$ , 60 s for each interval), and 5 cycles were carried out.

### **Conductivity test**

Before performing the conductivity test, the hydrogels were swollen in deionized water and the excess water on the hydrogel surface was removed using filter paper. Followed that, the hydrogel was transferred into a cylinder after exposed to air for 30 min. The conductivity of the hydrogels was measured by employing a digital 4-probe tester measurements.<sup>[6]</sup>

### **Mechanical properties of hydrogel**

Hydrogel samples were prepared into cylindrical shape ( $\sim 8 \text{ mm}$  high  $\times 1.0 \text{ mm}$  in diameter) for compression test at 25 °C. The test was investigated using a rheometer (Model DHR-2, TA Instruments) with a speed of 6 mm/min at 60% strain and then recovered to 0% strain with a speed of 6 mm/min. This cycle was repeated for 50 times to determine the compressive and

recovery properties. All these tests were employed more than 5 times.<sup>[7]</sup>

The mechanical tensile stress–strain evaluation was carried out by the uniaxial tensile test employing an materials test system (MTS Criterion 43; MTS Criterion) equipped with a 50 N tension sensor at room temperature. All the hydrogel samples were prepared into stripes (30 mm in length × 6 mm in width × 200 μm in thickness). The tensile strength and elongation at break were obtained at a crosshead rate of 2 mm/min.

### **Antioxidant efficiency of hydrogels**

The antioxidant efficiency of hydrogels was evaluated by the method of scavenging the stable 1, 1-diphenyl-2-picrylhydrazyl (DPPH) free radical.<sup>[8]</sup> The hydrogels were cut into homogenate by using tissue grinder. Afterwards, 100 μM DPPH and desired amount of HA-DA/rGO3 hydrogel samples (30 mg, 15 mg, 7.5 mg, 3.75 mg and 1.875 mg) were dispersed in 3.0 mL ethanol. The mixture was stirred and incubated in a dark place for half an hour. Next, the wavelength of DPPH was scanned by a UV–vis spectrophotometer. The degradation of DPPH was calculated by the following formula:

$$\text{DPPH scavenging \%} = \frac{A_B - A_H}{A_R} \times 100$$

where  $A_B$ ,  $A_H$  are the absorption of the blank (DPPH + ethanol) and the absorption of the hydrogel (DPPH +ethanol +hydrogel), respectively. The antioxidant efficiency of pure curcumin with the same amount of curcumin in the hydrogel was also tested.

### **Adhesive strength test of the hydrogel**

According to our previous work,<sup>[9, 10]</sup> the adhesive ability of the hydrogels to the host tissue was conducted by using fresh porcine skin. Briefly, the skin tissue was cut into 10 mm × 30 mm rectangle and then immersed into PBS before use. 100 μL of HA-DA/rGO hydrogel solutions were applied onto the surface of porcine skin and another skin was put onto the hydrogel solution. The adhesive area was 10 mm × 10 mm. Subsequently, the porcine skin was placed at room temperature for 2 h. The adhesion properties were tested using the lap

shear test on a Materials Test system (MTS Criterion 43, MTS Criterion) equipped with a 50 N load cell at a rate of 2 mm/min. All these tests were employed more than 5 times.

### **In vivo hemostatic ability test**

According to the reference,<sup>[11]</sup> a hemorrhaging liver mouse (Kunming mice, 20-30 g, female) were employed to evaluate the hemostatic potential of the HA-DA/rGO hydrogels. Briefly, by injecting 10 wt% chloral hydrate, a mouse was anesthetized and then fixed on a surgical corkboard. The liver of the mouse was exposed by abdominal incision, and serous fluid around the liver was carefully removed. A pre-weighted filter paper on a paraffin film was placed beneath the liver. Bleeding from the liver was induced using a 20 G needle with the corkboard tilted at about 30° and 50 µL of HA-DA/rGO3 hydrogel solution was immediately applied on the bleeding site using the syringe. Ten minutes' later, the weight of the filter paper with absorbed blood was measured and compared with a control group (no treatment after pricking the liver).

### **NIR irradiation enhanced in vitro and in vivo antibacterial performance of hydrogels**

The HA-DA/rGO hydrogel disks (5 × 5 × 5 mm) were prepared by using sterilized HA-DA solution and rGO@PDA suspensions under a sterile environment, and then equilibrated with sterilized Dulbecco's phosphate buffered saline (DPBS). 10 µL of bacterial suspension in sterilized DPBS ( $10^8$  CFU mL<sup>-1</sup>) was added onto the surface of the hydrogel disks (HA-DA/rGO0 and HA-DA/rGO3). Then, the hydrogel was exposed to NIR laser light (808 nm, 1.0 W/cm<sup>2</sup>) for varying periods from 0 to 1, 3, 5 and 10 min, respectively. 10 µL of bacterial suspension ( $10^8$  CFU mL<sup>-1</sup>) was used as a negative control, which was also exposed to NIR laser light (808 nm, 1.0 W/cm<sup>2</sup>). After allowing all the groups to contact with bacteria for preset time, 1 mL of sterilized DPBS was added into each well to re-suspend any bacterial survivor. Then, 10 µL of the above bacterial survivor resuspension was added onto agar plate, the colony-forming units on the agar plate were counted after incubated for 18 to 24 h at 37 °C.<sup>[12]</sup>

For the *in vivo* NIR irradiation enhanced antibacterial performance test, Female Kunming mice weighting 25-35 g and 5-6-week age were chosen. All mice were randomly divided into 4 groups including control, NIR irradiation, hydrogel HA-DA/rGO3 and hydrogel HA-DA/rGO3+NIR irradiation. Each group contained 5 mice. All mice were acclimatized for 1 week before surgery. For the surgery part, all procedures were performed under aseptic condition. After standard anesthesia procedure with intraperitoneal injection of chloral hydrate (0.3 mg/kg body weight), the dorsal region of mice above the tail but below the back were shaved to prepare for surgery. 7 mm diameter full thickness skin round wounds were created by a needle biopsy. After the removal of wound skin, all of the group were added with 10  $\mu$ L of *S. aureus* suspension ( $10^8$  CFU/mL). Then, all wounds were covered with Tegaderm<sup>TM</sup> film for 48 h.<sup>[13]</sup> When all of the mouse became infected, half of the mouse were covered with HA-DA/rGO3 hydrogel. And for the NIR irradiation group and HA-DA/rGO3+NIR irradiation group, wounds were exposed to NIR laser light (808 nm, 1.0 W/cm<sup>2</sup>) for 10 min. After all operations are completed, the samples were taken and dispersed in 5 mL of PBS by a tissue crusher, and then these samples contained PBS were diluted and cultured on LB agar plates to check the antibacterial activity.

### **In vitro drug release study**

200  $\mu$ L of HA-DA/rGO hydrogels loaded with desired amount of doxycycline (2 mg/mL) were prepared in a 4 mL centrifuge tube. After allowing complete gelation, the hydrogels formed and the drug was encapsulated in the hydrogels *in situ*. 3 mL of PBS with pH values of 7.4 was pipetted into each tube with shaking speed of 100 rpm at 37 °C. After a predetermined time, 1 mL of the release buffer was removed for further analysis. Subsequently, 1 mL of fresh buffer was added to the tube in order to maintain a constant volume.<sup>[14]</sup> The concentrations of the drugs released from hydrogels were analyzed by the UV-vis spectrophotometer (PerkinElmer Lambda 35). The  $\lambda_{\max}$  of doxycycline was 351 nm. In order to better understand the release mechanism of doxycycline from these hydrogels, the

release profiles were fitted by the Korsmeyer-Peppas equation:

$M_t/M_0 = k * t^n$ , where  $M_t$  and  $M_0$  correspond to the cumulative amount of drug released at time  $t$  and at equilibrium, respectively.  $k$  is the kinetic constant, and  $n$  is an exponent. Additionally, for determination of the exponent  $n$ , only the initial portion of the release curve ( $M_t/M_0 < 0.6$ ) was used. For cylindrical samples, when the diffusion exponent  $n$  was tested to be less than 0.45, the release mechanism could be described by Fickian diffusion.

### **Antibacterial activity of doxycycline encapsulated HA-DA/rGO hydrogel**

In this test, agar plates were inoculated with 100  $\mu$ L of the bacterial suspension ( $10^8$  CFU/mL). The samples were exposed to bacteria on solid media (nutrient agar), and the inhibition zone around each sample was measured and recorded as the antibacterial effect of doxycycline loaded HA-DA/rGO hydrogel. Hydrogels were placed on the agar plate and incubated at 37 °C for 24 h. The inhibition zone for bacterial growth was detected visually. After 24 h, the hydrogels were transferred to a new agar plate covered with bacteria and incubated for another 24 h. Subsequently, the above operation was repeated again until no inhibition zone appeared on the new agar plate.

### **Hemolytic activity test of the hydrogels**

Hemolysis activity assay was conducted according to reference.<sup>[15]</sup> Erythrocytes were separated by centrifugation (at 1,000 rpm) from the mice blood for 10 minutes. The obtained erythrocytes were washed three times with PBS buffer and then diluted to a final concentration of 5% (v/v) by PBS. Hydrogel (500  $\mu$ l) mixed with erythrocytes stock (500  $\mu$ l) was added to a 24-well microplate, then shaken in an incubator at 37 °C for 1 h with a shaking speed of 100 rpm. 0.1% Triton x-100 was used as the positive control while PBS buffer was used as the negative control. After that, the microplate well contents were centrifuged (at 1,000 rpm) for 10 minutes and the supernatant (100  $\mu$ L) was then introduced into a new 96-well microplate. The absorbance of the solution was read at 540 nm by a microplate reader (Molecular Devices). The hemolysis percentage was calculated from the relation: Hemolysis



(%) =  $[(A_p - A_b)/(A_t - A_b)] \times 100\%$ , where  $A_p$  was the absorbance value for a copolymer solution with confirmed concentration.  $A_t$  was the absorbance value for the Triton x-100 positive control and  $A_b$  was the absorbance value for PBS.

### **Cytocompatibility evaluation of the hydrogels**

The cytotoxicity of hydrogels was measured by employing a direct contact test between hydrogels and L929 cells.<sup>[4, 16]</sup> As described before in the section of hydrogel preparation, dry HA-DA and rGO@PDA was sterilized at 60 °C for 12 h. The solution of H<sub>2</sub>O<sub>2</sub> and HRP was sterilized by filtration (0.22 μm filter, Millipore) for 10 seconds equivoluminally. After mixing, the mixture was poured into a sterile Petri dish to form a hydrogel film with about 1.5 mm thickness at 37 °C in CO<sub>2</sub> incubator. Then hydrogel film was cut into 5 mm diameter disks using a Harris Micro-Punch (Harris Uni-Core™, USA) and the dulbecco's modified eagle medium (DMEM) (Gibco) supplemented with 10% fetal bovine serum (Gibco), 1.0 × 10<sup>5</sup> U/L penicillin (Hyclone) and 100 mg/L streptomycin (Hyclone) was used as the complete growth medium. L929 cells were seeded in 96-well plate at a density of 20000 cells/well. After cultured for 24 h, the hydrogel disks were introduced into the wells. The cell proliferation and viability under the hydrogel was evaluated by alamarBlue® assay and LIVE/DEAD® Viability/Cytotoxicity Kit assay, respectively.

After being co-incubated for 1, 3 and 5 days, the hydrogel disks and medium were removed and 10 μL of alamarBlue® reagent in 100 μL complete growth medium was then added into each well. The plate was incubated for 4 h in a humidified incubator containing 5% CO<sub>2</sub> at 37 °C. After that, 100 μL of the medium in each well was transferred into a 96-well black plate (Costar). Fluorescence was read using 560 nm as the excitation wavelength and 600 nm as the emission wavelength using a microplate reader (Molecular Devices) according to the manufacturer's instructions. Cells seeded on TCP without hydrogel disc served as the positive control group. Tests were repeated four times for each group. Cell adhesion and viability were observed under an inverted fluorescence microscope (IX53, Olympus). The cell viability was

evaluated by alamarBlue® assay after cultured for 24 h.

### **In vivo wound healing in a full-thickness skin defect model**

Our animal experiments were approved by the institutional review board of Xi'an Jiaotong University. Female Kunming mice weighting 25-35 g and 5-6-week age were used for studies. All mice were randomly divided into 4 groups including Tegaderm™ film (control), hydrogel HA-DA/rGO0, hydrogel HA-DA/rGO3 and hydrogel HA-DA/rGO3/Doxy. Each group contained 15 mice. All mice were acclimatized for 1 week before surgery. For the surgery part, all procedures were performed under aseptic condition. After standard anesthesia procedure with intraperitoneal injection of chloral hydrate (0.3 mg/kg body weight), the dorsal region of mice above the tail but below the back were shaved to prepare for surgery. 7 mm diameter full thickness skin round wounds were created by a needle biopsy. After the removal of wound skin, control wounds were added with 50 µL of PBS then dressed with Tegaderm™ film (3M Health Care, USA), and hydrogel group wounds were added with 50 µL of hydrogel HA-DA/RGO0, hydrogel HA-DA/rGO3 or hydrogel HA-DA/rGO3/Doxy. All tissues were collected on each 5 mice in 3 groups on 3rd, 7th, 14th day. All samples were stored at -80 °C before analysis. The regeneration process of wounds was assessed by wound area monitoring. For wound area monitoring, on the 3rd, 7th, 14th day, the mice in each group were performed standard anesthesia procedure with intraperitoneal injection of chloral hydrate (0.3 mg/kg body weight), then wound area were measured by tracing the wound boundaries on plotting papers. All results were analyzed by one-way ANOVA test.<sup>[17]</sup>

For the biochemical analysis, on the 3rd, 7th, 14th day, the samples were collected and made into disc-shaped tissue (diameter = 1 cm), and collagen amount was evaluated by estimating hydroxyproline content using a commercial kit (Jiancheng Bioengineering, China). All operations were followed manufacturer's instruction.<sup>[11]</sup>

### **Histology and immunohistochemistry**

For evaluation of epidermal regeneration and inflammation in wound area, samples collected

on the 3rd, 7th, 14th day were fixed with 4% paraformaldehyde for 1 h, then embedded in paraffin and cross sectioned to 4  $\mu\text{m}$  thickness slices, and then stained with Haematoxylin-Eosin (Beyotime, China). All slices were analyzed and photo-captured by microscope ((IX53, Olympus, Japan). The regenerated skins from the wound site were also excised on 3, 7, and 14 days for immunofluorescence staining. The fixed and frozen sections were stained with Anti-CD31 antibody (abcam) and TNFA Ab (Affinity Biosciences), respectively. FITC-conjugated goat anti-mouse IgG (cwbiotech) and FITC-conjugated goat anti-rabbit IgG (cwbiotech) were used as the secondary antibody to reveal CD31 and TNF- $\alpha$  expression. The nuclei were stained with DAPI containing mounting solution. Slides were observed under an inverted fluorescence microscope (IX53, Olympus).

## Results and discussion

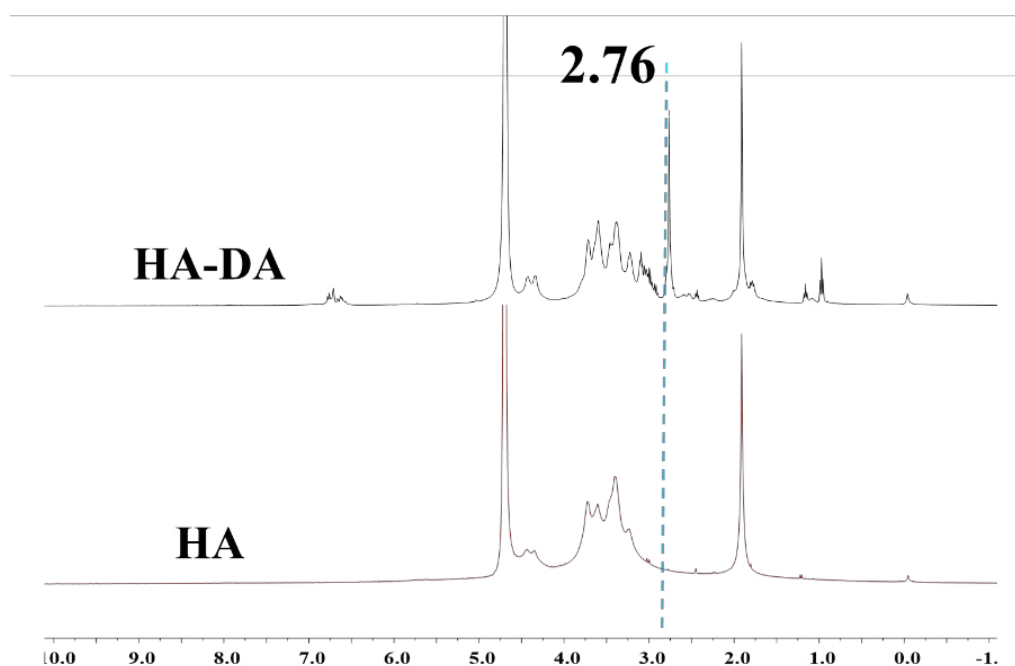


**Figure S1.**  $^1\text{H-NMR}$  data of HA and HA-DA

The protons in the catechol ring newly appeared at 6.7 ppm, and the proton peak at 2.76 ppm was due to a  $-\text{CH}_2-$  group close to the catechol ring. The results confirmed that the conjugation of dopamine to HA was successful.<sup>[18]</sup>

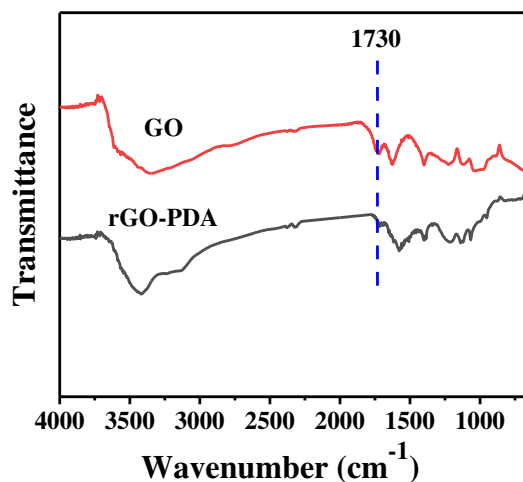


**Figure S2.** FT-IR of GO and rGO@PDA.

The change of peak at  $1227\text{ cm}^{-1}$  corresponds to the C–N vibration. The bands at  $2962$  and  $2873\text{ cm}^{-1}$  are ascribed to C–H stretching vibrations of methyl or methylene groups. It confirmed the polymerization of dopamine and the presence of PDA layer on the rGO. Importantly, the disappearance of the C–O peak at  $1730\text{ cm}^{-1}$  compared to GO provided a direct indication of the reduction of GO.<sup>[19]</sup>

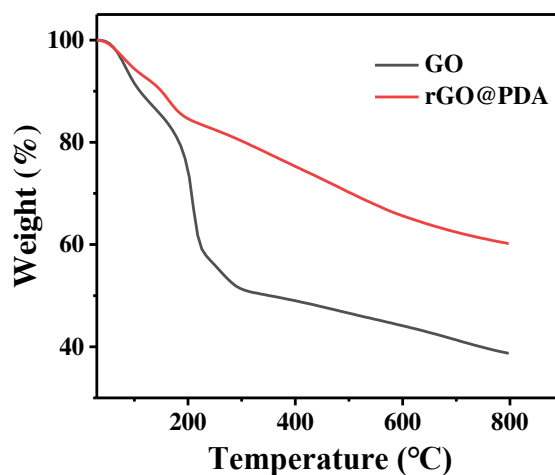


**Figure S3.** TGA of GO and rGO@PDA.

There is a significant weight loss of GO before  $200\text{ °C}$ , which is due to the evaporation of interlamellar water and the decomposition of labile oxygen. After modification with PDA, the weight loss of rGO@PDA decreased. This loss is attributed to the enhanced thermal stability of GO.<sup>[20]</sup>

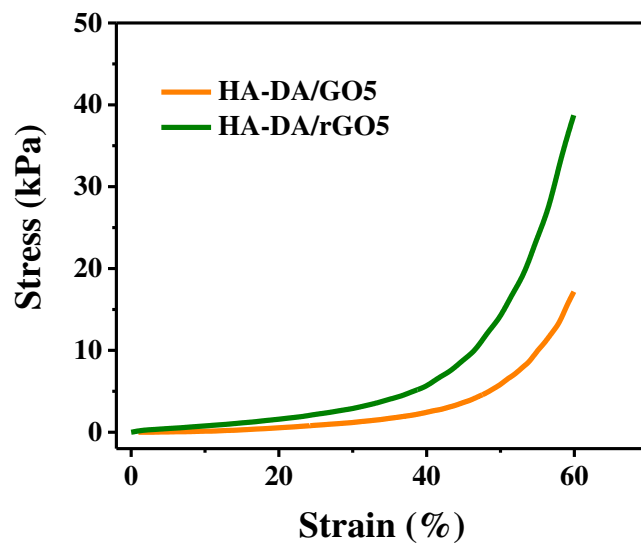


**Figure S4.** The uniaxial compression stress–strain curves of the HA-DA/GO5 and HA-DA/rGO5 hydrogel.

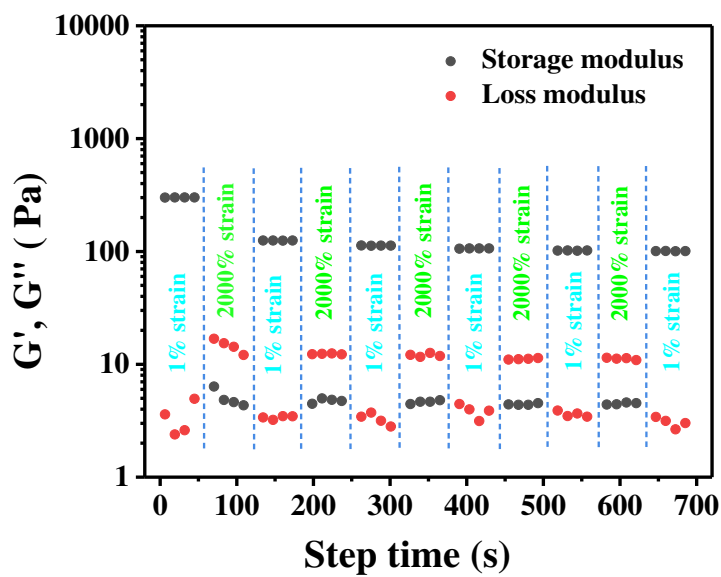


**Figure S5.** The rheological properties of the hydrogel when alternate step strain switched from 1% to 2000%.

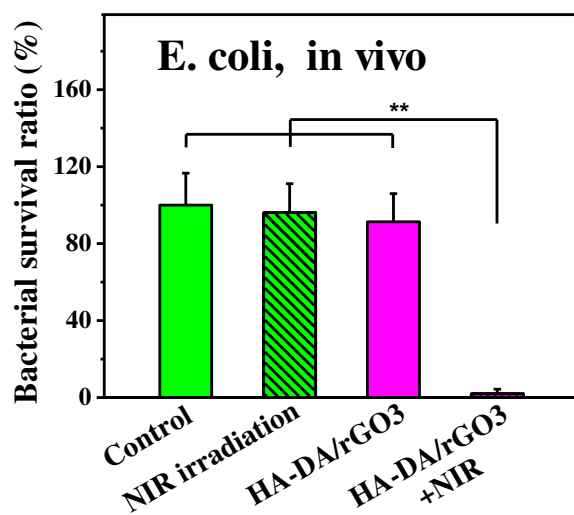


**Figure S6.** NIR irradiation enhanced in vivo antibacterial performance of hydrogels for *E. coli*.

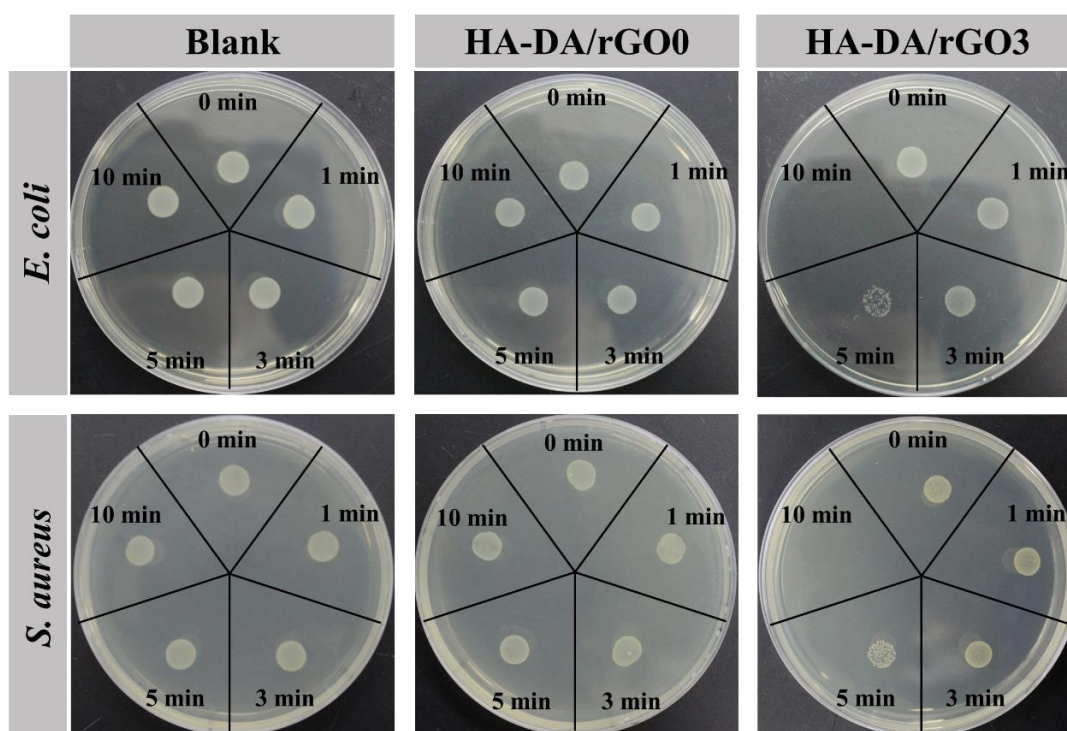


**Figure S7.** Photographs of in vitro photo-thermal antibacterial performance of HA-DA/rGO0 and HA-DA/rGO3 hydrogel.

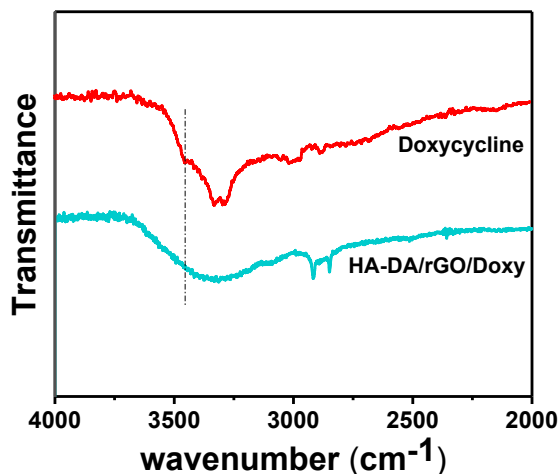


**Figure S8.** FT-IR spectra of doxycycline and HA-DA/rGO/Doxy hydrogel.

## References

- [1] S. R. Shin, C. Zihlmann, M. Akbari, P. Assawes, L. Cheung, K. Zhang, V. Manoharan, Y. S. Zhang, M. Yuksekkaya, K. T. Wan, M. Nikkhah, M. R. Dokmeci, X. S. Tang, A. Khademhosseini, *Small* **2016**, 12, 3677.
- [2] L. Q. Xu, W. J. Yang, K.-G. Neoh, E.-T. Kang, G. D. Fu, *Macromolecules* **2010**, 43, 8336.
- [3] Y. Wu, L. Wang, B. Guo, Y. Shao, P. X. Ma, *Biomaterials* **2016**, 87, 18.
- [4] X. Zhao, R. Dong, B. Guo, P. X. Ma, *Acs Appl. Mater. Inter.* **2017**, 9, 29595.
- [5] J. Qu, X. Zhao, P. X. Ma, B. Guo, *Acta Biomater.* **2017**, 58, 168.
- [6] Z. Deng, Y. Guo, X. Zhao, P. X. Ma, B. Guo, *Chem. Mater.* **2018**, 30, 1729.
- [7] X. Zhao, B. Guo, H. Wu, Y. Liang, P. X. Ma, *Nat. Commun.* **2018**, 9, 2784.
- [8] R. Gharibi, H. Yeganeh, A. Rezapour-Lactoe, Z. M. Hassan, *Acs Appl. Mater. Inter.* **2015**, 7, 24296.
- [9] R. Dong, X. Zhao, B. Guo, P. X. Ma, *Acs Appl. Mater. Inter.* **2016**, 8, 17138.
- [10] Y. Liang, X. Zhao, P. X. Ma, B. Guo, Y. Du, X. Han, *J. Colloid. Interf. Sci.* **2018**.
- [11] J. Qu, X. Zhao, Y. Liang, T. Zhang, P. X. Ma, B. Guo, *Biomaterials* **2018**, 183, 185.
- [12] M.-C. Wu, A. R. Deokar, J.-H. Liao, P.-Y. Shih, Y.-C. Ling, *ACS nano* **2013**, 7, 1281.

- [13] H. Xu, Z. Fang, W. Tian, Y. Wang, Q. Ye, L. Zhang, J. Cai, *Adv. Mater.* **2018**, e1801100.
- [14] C. J. Tormos, C. Abraham, S. V. Madihally, *Drug Deliv. Transl. Re.* **2015**, 5, 575.
- [15] A. Sasidharan, L. S. Panchakarla, A. R. Sadanandan, A. Ashokan, P. Chandran, C. M. Girish, D. Menon, S. V. Nair, C. Rao, M. Koyakutty, *Small* **2012**, 8, 1251.
- [16] X. Zhao, P. Li, B. Guo, P. X. Ma, *Acta Biomater.* **2015**, 26, 236.
- [17] Z. Fan, B. Liu, J. Wang, S. Zhang, Q. Lin, P. Gong, L. Ma, S. Yang, *Adv. Funct. Mater.* **2014**, 24, 3933.
- [18] A. I. Neto, A. C. Cibrao, C. R. Correia, R. R. Carvalho, G. M. Luz, G. G. Ferrer, G. Botelho, C. Picart, N. M. Alves, J. F. Mano, *Small* **2014**, 10, 2459.
- [19] S.-K. Li, Y.-X. Yan, J.-L. Wang, S.-H. Yu, *Nanoscale* **2013**, 5, 12616.
- [20] J. Hu, X. Jia, C. Li, Z. Ma, G. Zhang, W. Sheng, X. Zhang, Z. Wei, *J Mater. Sci.* **2014**, 49, 2943.